VII. QCD, jets and gluons

Quantum Chromodynamics (QCD)

❖ *Quantum Chromodynamics (QCD)* is the theory of strong interactions.

➔ Interactions are carried out by a <u>massless</u> spin-1 particle – *gauge boson*

➔ In quantum electrodynamics (QED) gauge bosons are photons, in QCD – *gluons*

➔ Gauge bosons couple to conserved charges: photons in QED – to electric charges (Q), and gluons in QCD – to colour charges: colour hypercharge (Y^c) and colour isospin charge (I_3^c).

➔ The strong interaction acts the same on u,d,s,c,b and t quarks because the strong interaction is **flavour-independent.**

REMINDER:

In the quark model we have introduced flavour hypercharge (Y) and flavour isospin (I_3) in addition to the electric charge (Q).

	Q	Y	I_3		Q	Y	I_3
d	-1/3	1/3	-1/2	$\bar{d}$	1/3	-1/3	1/2
u	2/3	1/3	1/2	$\bar{u}$	-2/3	-1/3	-1/2
s	-1/3	-2/3	0	$\bar{s}$	1/3	2/3	0
c	2/3	4/3	0	$\bar{c}$	-2/3	-4/3	0
b	-1/3	-2/3	0	$\bar{b}$	1/3	2/3	0
t	2/3	4/3	0	$\bar{t}$	-2/3	-4/3	0

In quantum chromodynamics we introduce in a similar fashion colour hypercharge (Y^c) and colour isospin charge (I_3^c).

	Y^c	I_3^c		Y^c	I_3^c
r	1/3	1/2	$\bar{r}$	-1/3	-1/2
g	1/3	-1/2	$\bar{g}$	-1/3	1/2
b	-2/3	0	$\bar{b}$	2/3	0

❖   Gluons carry colour charges themselves !

$I_3^C = 1/2$ $Y^C = 1/3$ u   u $I_3^C = 0$ $Y^C = -2/3$

$I_3^C = 1/2$ $Y^C = 1$

$I_3^C = 0$ $Y^C = -2/3$ s   s $I_3^C = 1/2$ $Y^C = 1/3$
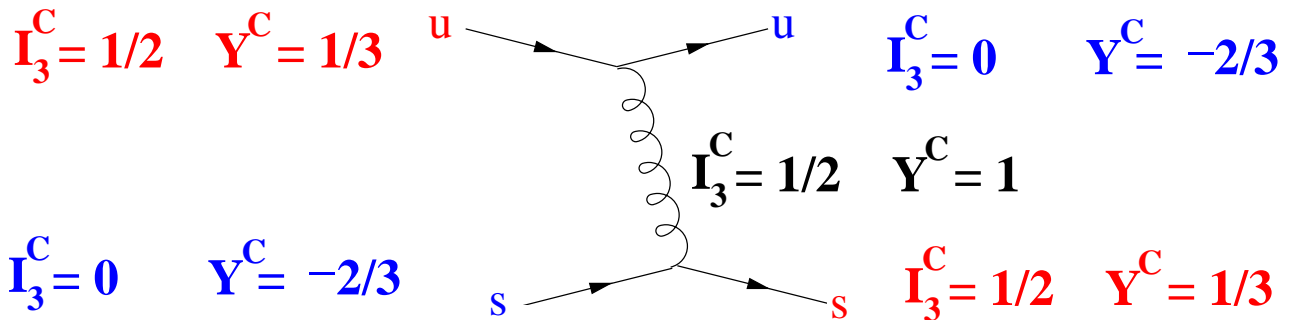
<div align="center">Figure 58:   Gluon exchange between quarks.</div>

The colour quantum numbers of the gluon in the figure above are:

$$I_3^C = I_3^C(r) - I_3^C(b) = \frac{1}{2} \tag{86}$$

$$Y^C = Y^C(r) - Y^C(b) = 1$$

Gluon colour wavefunctions:

$\chi_{g1}^C = r\,\bar{g}$	$I_3^C = 1$	$Y^C = 0$
$\chi_{g2}^C = \bar{r}\,g$	$I_3^C = -1$	$Y^C = 0$
$\chi_{g3}^C = r\,\bar{b}$	$I_3^C = 1/2$	$Y^C = 1$
$\chi_{g4}^C = \bar{r}\,b$	$I_3^C = -1/2$	$Y^C = -1$
$\chi_{g5}^C = g\,\bar{b}$	$I_3^C = -1/2$	$Y^C = 1$
$\chi_{g6}^C = \bar{g}\,b$	$I_3^C = 1/2$	$Y^C = -1$
$\chi_{g7}^C = 1/\sqrt{2}\,(g\,\bar{g} - \bar{r}\,r)$	$I_3^C = 0$	$Y^C = 0$
$\chi_{g8}^C = 1/\sqrt{6}\,(g\,\bar{g} - r\,\bar{r} - 2\,b\,\bar{b})$	$I_3^C = 0$	$Y^C = 0$

❖ Gluons can couple to other gluons since gluons carry colour charge !

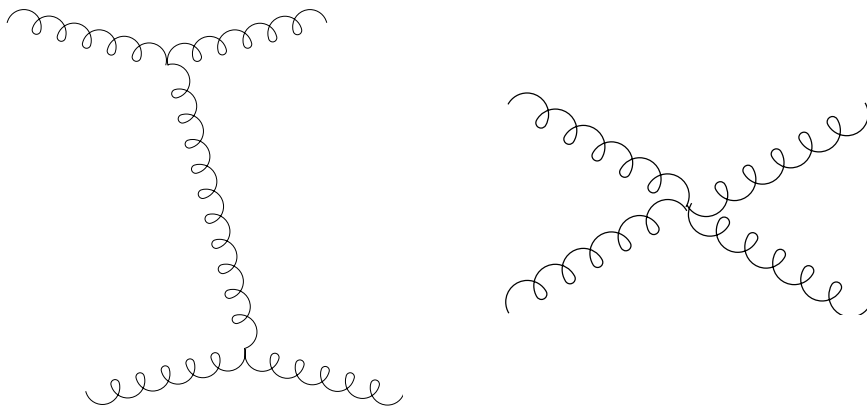Figure 59:   Lowest-order contributions to gluon-gluon scattering.

➔ All observed states (all mesons and baryons) have zero colour charge - colour confinement.

➔ Gluons does not exist as free particles since they have colour charge.

➔ Bound colourless states of gluons are called *glueballs* (not detected experimentally yet).

❖   The principle of asymptotic freedom:

➔   At short distances the strong interactions are weaker $\Rightarrow$ quarks and gluons are essentially free particles $\Rightarrow$ the interaction can be described by the lowest order diagrams.

➔   At large distances the strong interaction gets stronger $\Rightarrow$ the interaction can be described by high-order diagrams.
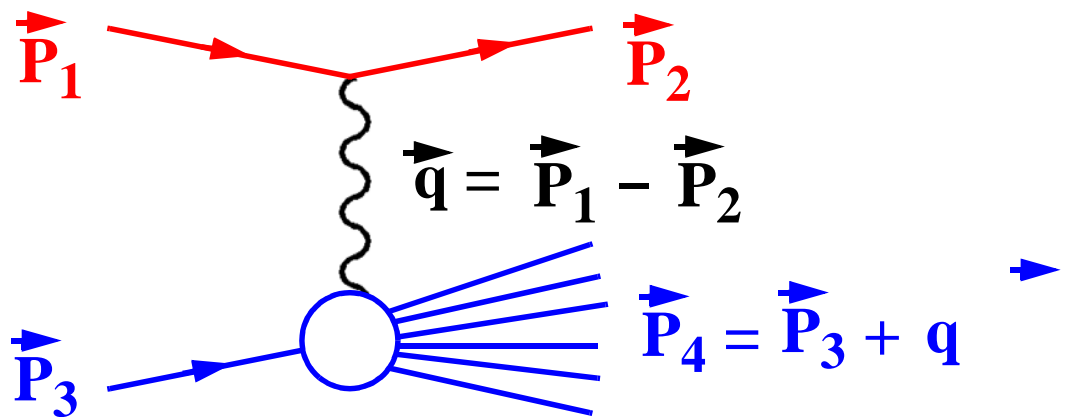
➔   The quark-antiquark potential is:

$$V(r) = -\frac{4}{3}\frac{\alpha_s}{r} \qquad (r < 0,1\,fm)$$
$$V(r) = \lambda r \qquad\qquad (r \geq 1fm)$$

where α_s is the strong coupling constant and *r* the distance between the quark and the antiquark.

➔   Due to the complexity of high-order diagrams, the very process of confinement can not be calculated analytically $\Rightarrow$ only numerical models are available.

VARIABLES

$$\vec{q} = \vec{P_1} - \vec{P_2}$$

$$\vec{P_4} = \vec{P_3} + q$$

where $\vec{P}$ and $\vec{q}$ are energy-momentum four vectors:

$$\vec{P} = (E, \bar{p}) = (E, p_x, p_y, p_z)$$

$$\vec{q} = (E_q, \bar{q}) = \vec{P_1} - \vec{P_2} = (E_1 - E_2, \overline{P_1} - \overline{P_2})$$

the momentum and energy transfer is:

$$q = |\bar{q}| = |\overline{P_1} - \overline{P_2}|$$

$$\nu = E_q = E_1 - E_2$$

(where E and P are in the restframe of particle 3).

The energy-momentum transfer is given by:

$$Q^2 = -\vec{q} \cdot \vec{q} = -(\vec{P_1} - \vec{P_2})^2$$

$$Q^2 = \bar{q} \cdot \bar{q} - E_q^2 = (\overline{P_1} - \overline{P_2})^2 - (E_1 - E_2)^2$$

This can be regarded as the invariant mass of the exchanged gauge boson since the squared mass of a particle is given by $M^2 = \vec{P} \cdot \vec{P}$

The invariant mass of the hadrons is given by:

$$W^2 = \vec{P_4} \cdot \vec{P_4} = (\vec{P_3} + \vec{q})^2$$

The strong coupling constant

❖   The strong coupling constant α_s is the analogue in QCD of α_{em} and it is a measure of the strength of the interaction.

➔ α_s is not a true constant but a "running constant" since it decreases with increasing Q^2.

➔   In leading order of QCD, α_s is given by

$$\alpha_s \; = \; \frac{12\pi}{(33 - 2N_f)\,ln(Q^2/\Lambda^2)} \qquad (87)$$

Here N_f is the number of allowed quark flavours, and $\Lambda \approx 0.2$ GeV is the QCD scale parameter which has to be defined experimentally.
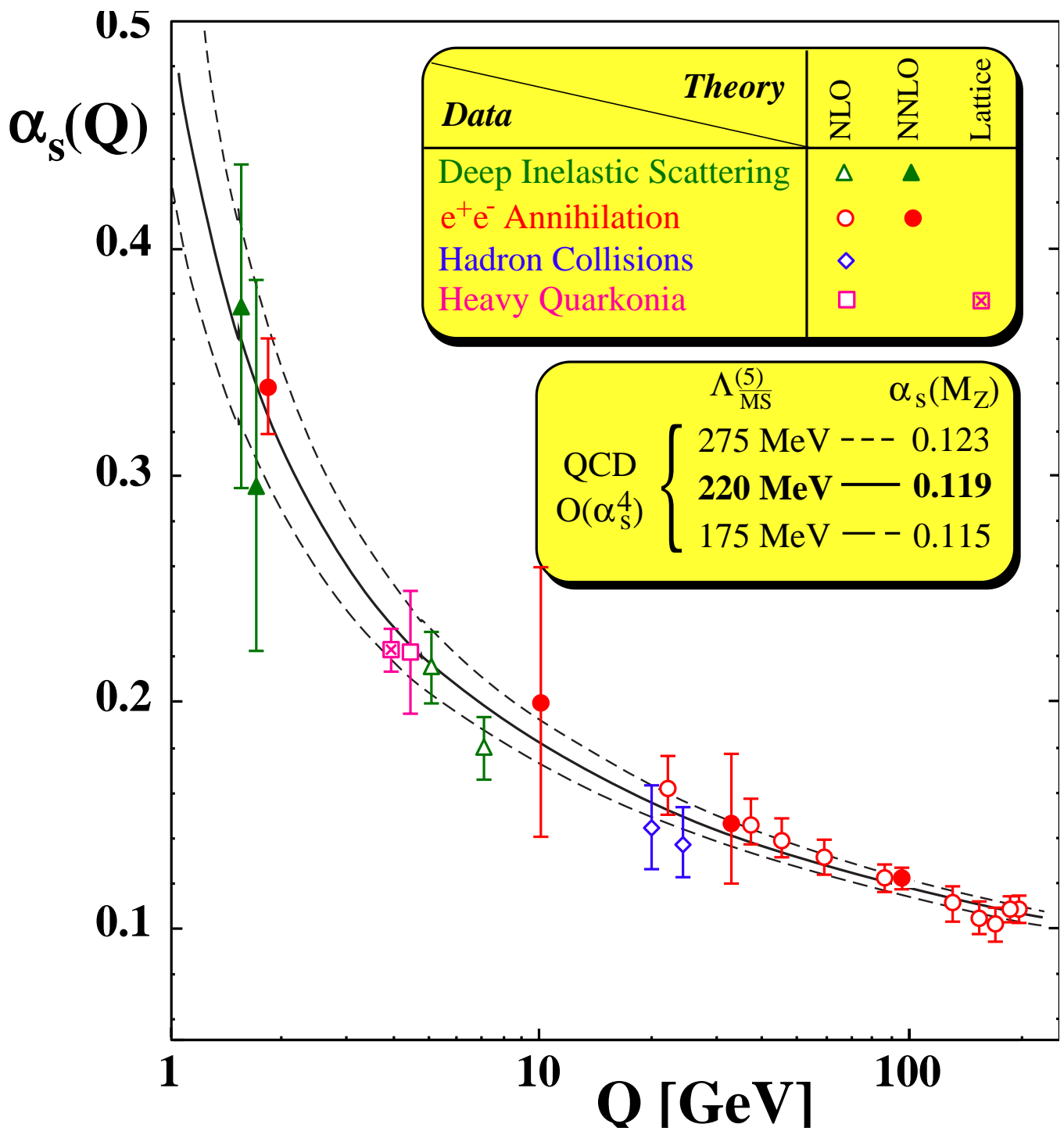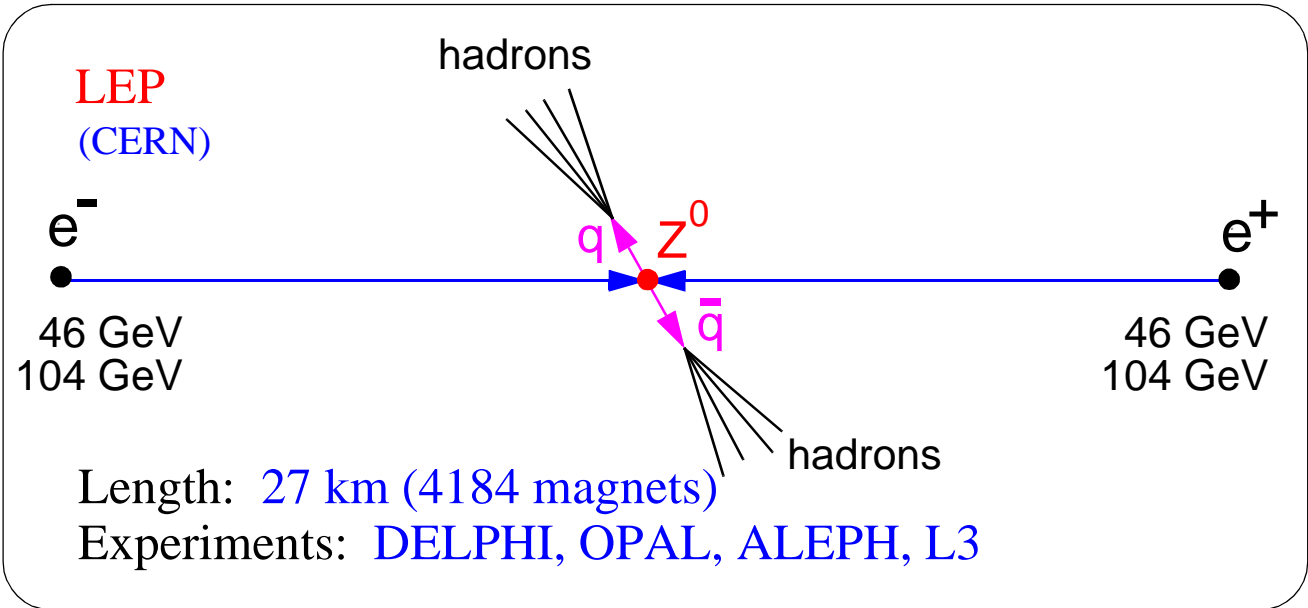
Figure 60:   The running of the strong coupling constant.

Different types of accelerators

LEP
(CERN)

e⁻

46 GeV
104 GeV

q   Z⁰   q̄

hadrons

hadrons

e⁺

46 GeV
104 GeV

Length: 27 km (4184 magnets)
Experiments: DELPHI, OPAL, ALEPH, L3

HERA
(DESY)

e⁺

30 GeV

e⁺

γ

hadrons

q̄
g
q̄
g
q̄
g

p

Length: 6 km (1650 magnets)
Experiments: H1, ZEUS

920 GeV

TEVATRON
(FERMILAB)

q
g
q
g
q
g

p

1000 GeV

hadrons

g

hadrons

q̄
g
q̄
g
q̄
g

p̄

1000 GeV

Length: 6 km (990 magnets)
Experiments: CDF, D0
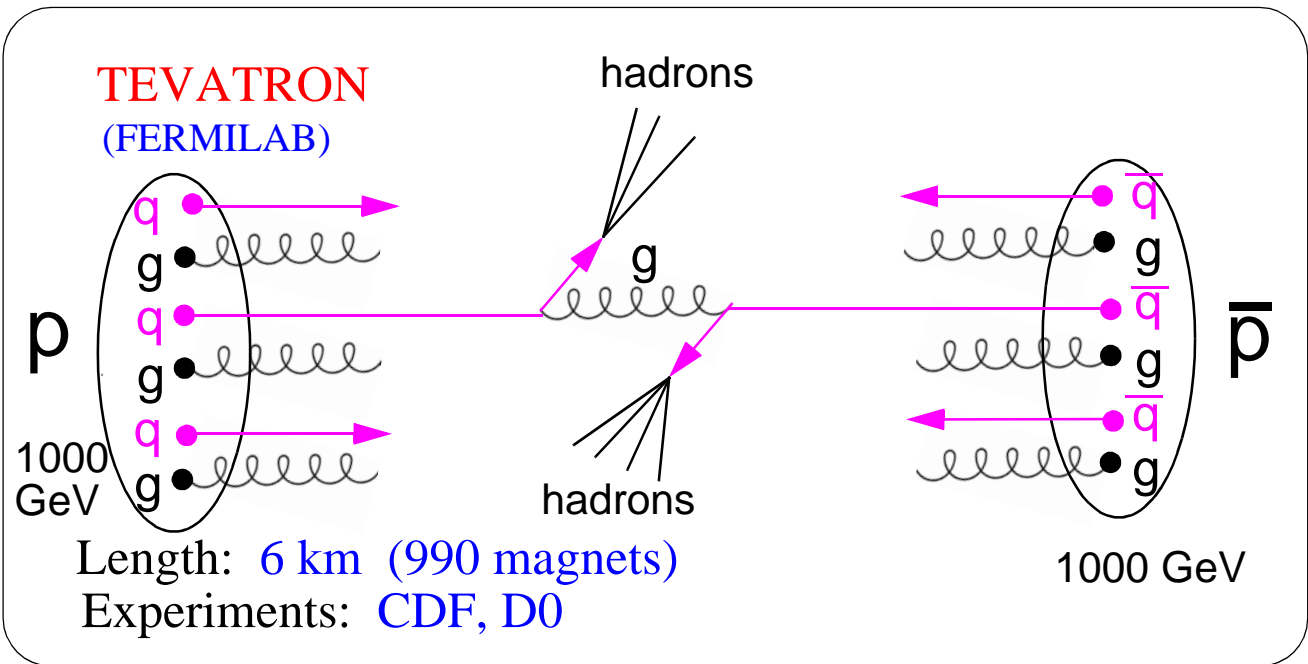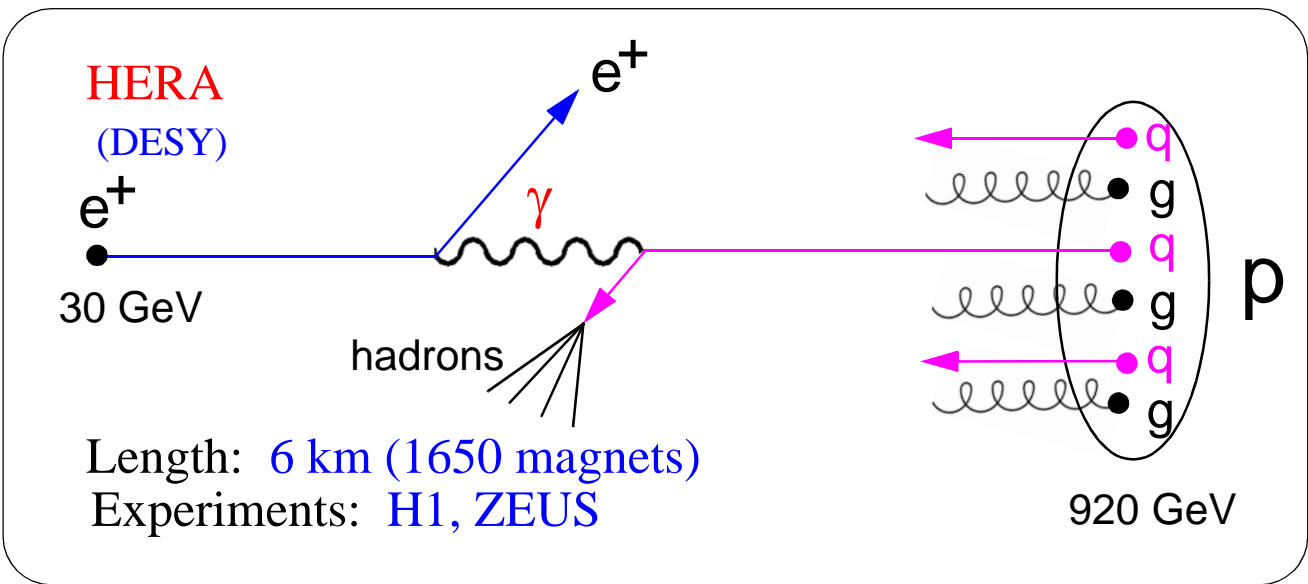
Electron-positron annihilation

A clean process with which to study QCD is:

$$e^+ + e^- \rightarrow \gamma^* \rightarrow \text{hadrons} \qquad (88)$$
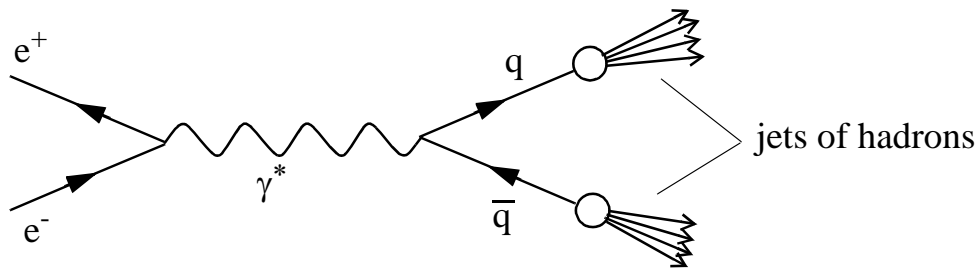
Figure 61:   e$^+$e$^-$ annihilation into hadrons.
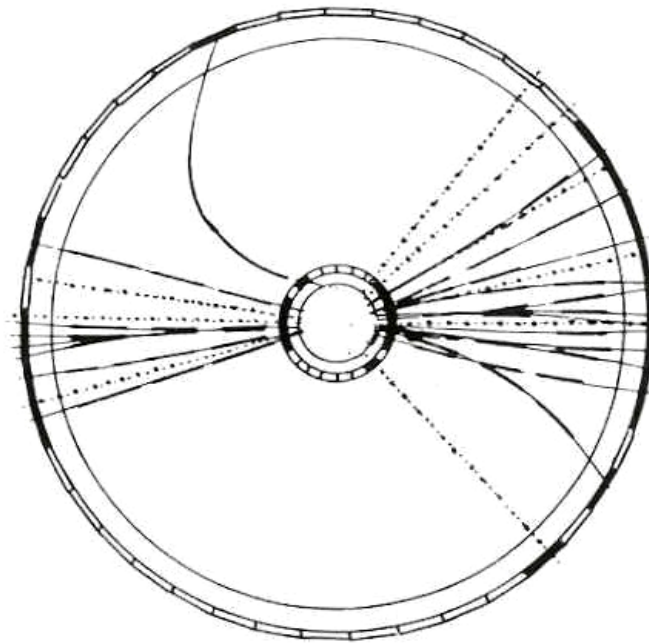
Figure 62:   An e$^+$e$^-$ annihilation event in which two quark jets were created (the event was recorded by the JADE experiment at DESY).

❖   In the lowest order e^+e^- annihilation process, a photon or a Z^0 is produced which converts into a quark-antiquark pair.

➔   The quark and the antiquark *fragment* into observable hadrons.

➔   Since the quark and antiquark momenta are equal and counterparallel, hadrons are produced in two *jets* of equal energies going in opposite direction.

➔   The direction of a jet reflects the direction of the corresponding quark.

➡ The total cross-section of $e^+e^- \to hadrons$ is often expressed as:

$$R \equiv \frac{\sigma(e^+e^- \to hadrons)}{\sigma(e^+e^- \to \mu^+\mu^-)}$$

The cross section for muon production and hadron production is the same if the number of quark flavours and colours are taken into account:

$$R = N_c \sum e_q^2$$

➡ Here $N_c = 3$ is the number of colours and e_q is the charge of the quarks.

➡ If $\sqrt{s} < m_\psi$ then

$$R = N_c(e_u^2 + e_d^2 + e_s^2) = 3\left((-1/3)^2 + (-1/3)^2 + (2/3)^2\right) = 2$$

If $\sqrt{s} < m_\Upsilon$ then $R = N_c(e_u^2 + e_d^2 + e_s^2 + e_c^2) = 10/3$ and

If $\sqrt{s} > m_\Upsilon$ then $R = N_c(e_u^2 + e_d^2 + e_s^2 + e_c^2 + e_b^2) = 11/3$

➔   If the radiation of hard gluons is taken into account, an extra factor proportional to α_s has to be added:

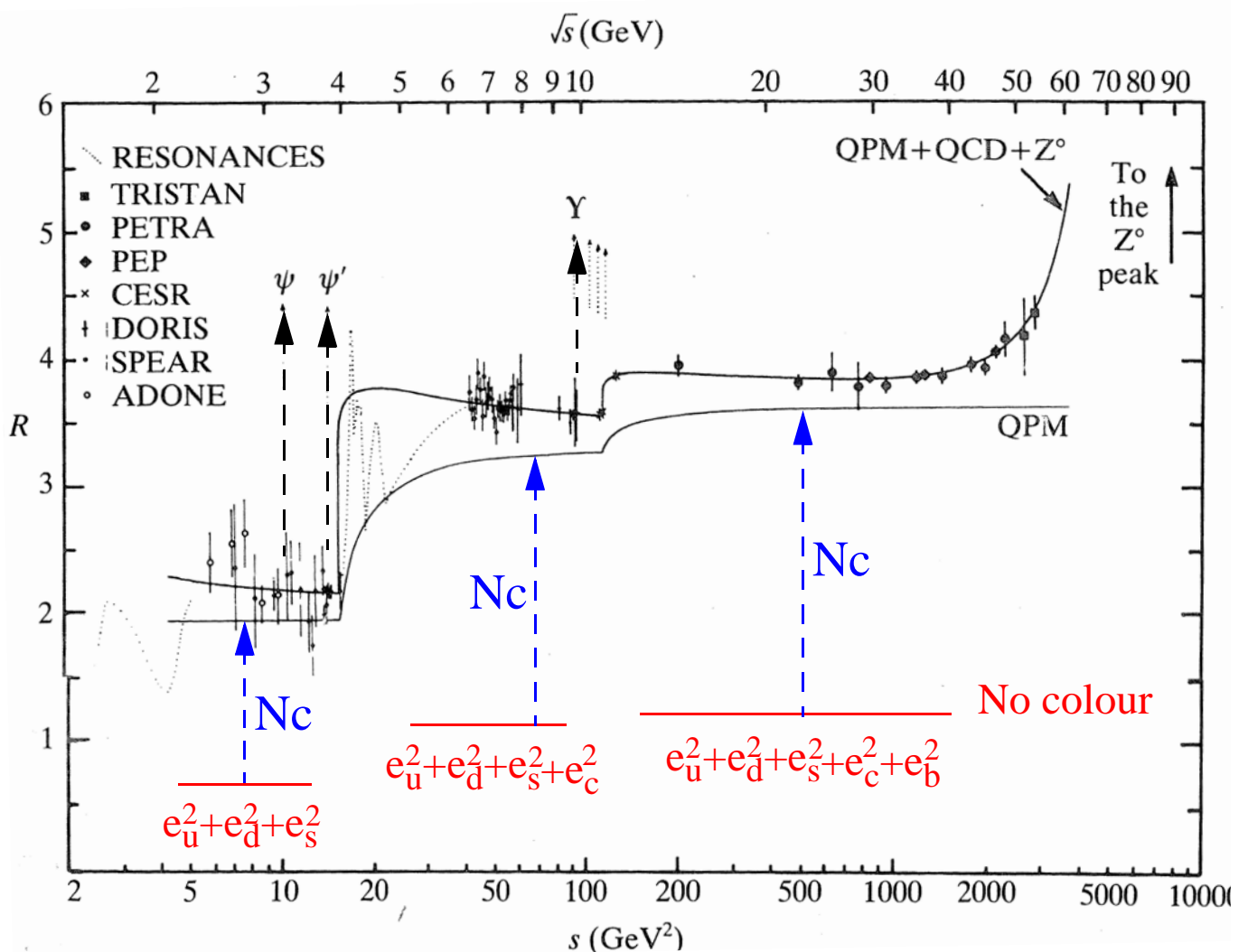$$R = 3\sum_q e_q^2\left(1 + \frac{\alpha_s(Q^2)}{\pi}\right)$$

Figure 63: The measured R-value and the predicted R-value for different theoretical assumptions.

❖ A study of the angular distribution of the jets give information about the spin of the quarks.

➔ The angular distribution of the process

$e^+ + e^- \to \gamma^* \to \mu^+ + \mu^-$ is given by:

$$\frac{d\sigma}{d\cos\theta}(e^+e^- \to \mu^+\mu^-) = \frac{\pi\alpha^2}{2Q^2}(1 + \cos^2\theta)$$

where θ is the production angle with respect to the direction of the colliding electrons.

➔ If quarks have spin 1/2 they should have the following angular distribution:

$$\frac{d\sigma}{d\cos\theta}(e^+e^- \to q\bar{q}) = N_c e_q^2 \frac{\pi\alpha^2}{2Q^2}(1 + \cos^2\theta)$$

where e_q is the fractional charge of a quark and $N_c = 3$ is the number of colours.

➔ If quarks have spin 0 the angular distribution should be:

$$\frac{d\sigma}{d\cos\theta}(e^+e^- \to q\bar{q}) = N_c e_q^2 \frac{\pi\alpha^2}{2Q^2}(1 - \cos^2\theta)$$
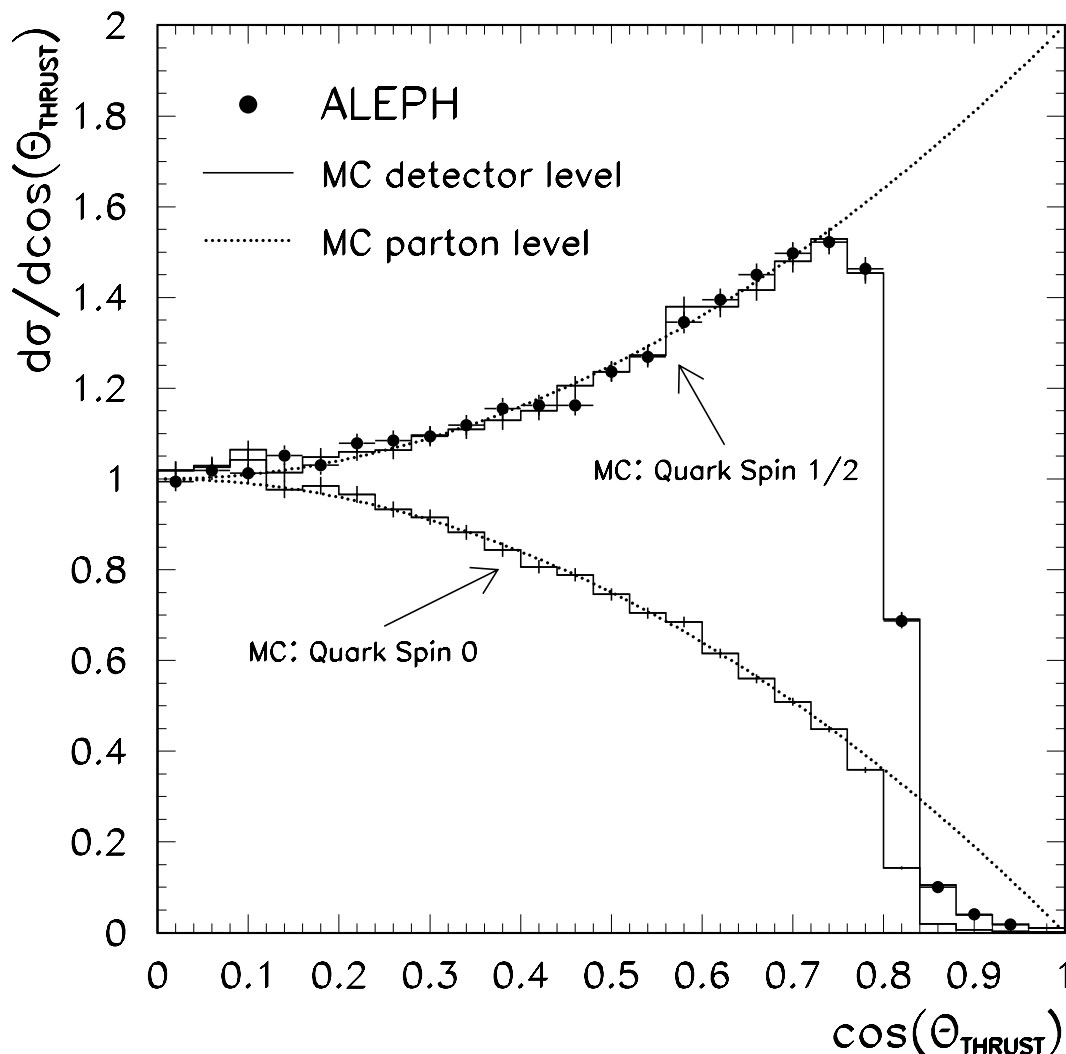
Figure 64:   The angular distribution of the quark jet in e^+e^- annihilations, compared with models.

➔   The experimentally measured angular dependence of jets is clearly following$(1+\cos^2\theta)$ $\Rightarrow$ jets are associated with spin-1/2 quarks.

➔ If a high-momentum (hard) gluon is emitted by a quark or antiquark, it fragments to a jet of its own, which leads to a three-jet event:
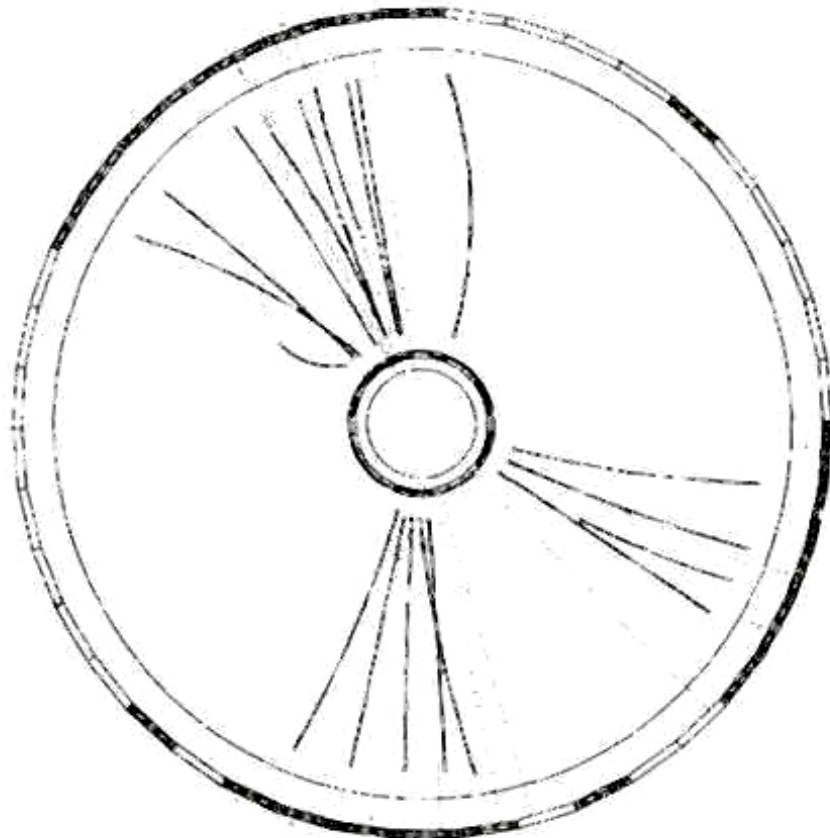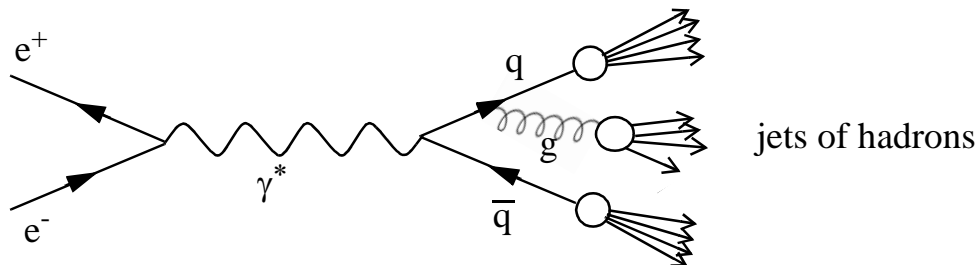

Figure 65: A three-jet event in an e⁺e⁻ annihilation as seen by the JADE experiment.

❖   The probability for a quark to emit a gluon is proportional to α_S and by comparing the rate of two-jet and three-jet events one can determine α_S.

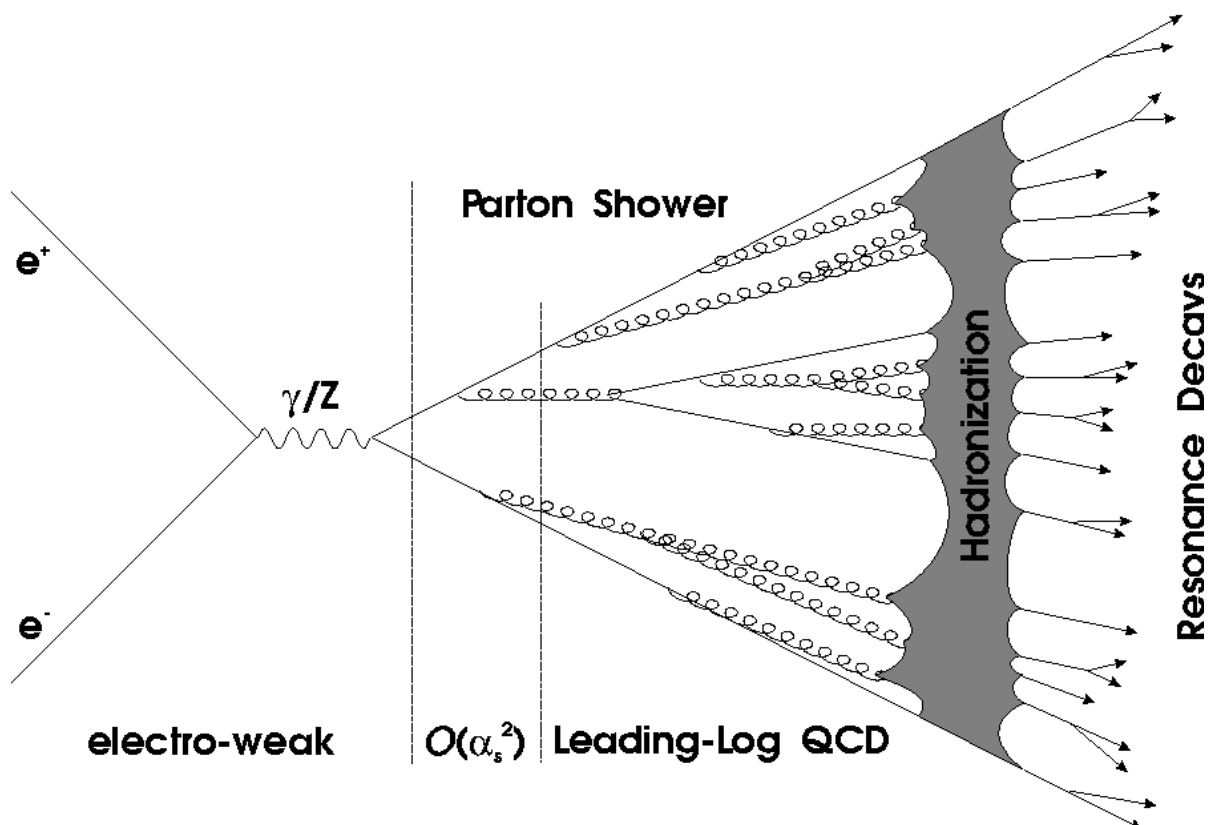➔ $\alpha_S = 0.15 \pm 0.03$ for E_{CM}=30 to 40 GeV

Figure 66: The principal scheme of hadron production in e⁺e⁻ annihilations. Hadronization (= fragmentation) begins at distances of order 1 fm between the partons.

❖   By measuring angular distributions of jets one can confirm models where gluons are spin-1 bosons. This is done by measuring:

$$cos\,\phi = \frac{sin\,\theta_2 - sin\,\theta_3}{sin\,\theta_1}$$

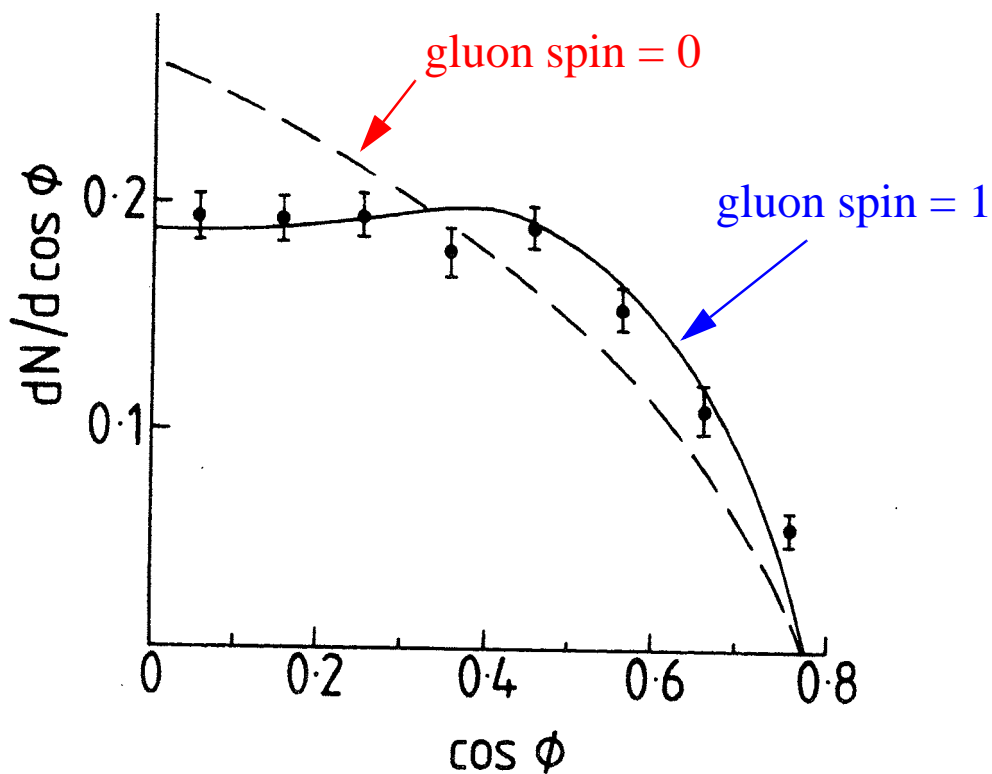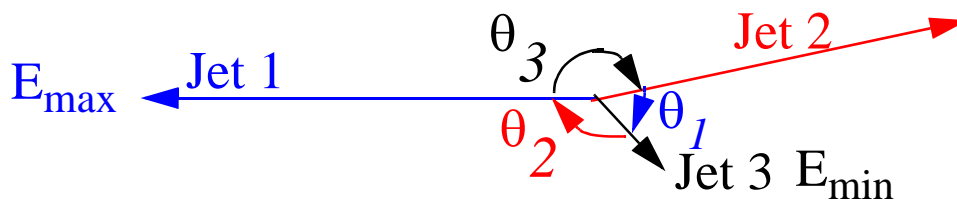where the angles are described below:

Figure 67:   An angular distribution of jets compared to QCD calculations with a spin 0 and a spin 1 gluon.

Elastic electron-proton scattering

❖   Beams of leptons are good tools for investigating the properties of hadrons since leptons have no substructure.

➔   Elastic lepton-hadron scattering can be used to measure the size of the hadron.

➔   Elastic scattering means that the same type of particles goes into and comes out of the scattering process.

$$\vec{P}_1 \quad \textbf{lepton} = e \text{ or } \mu \quad \vec{P}_2$$

$$\textbf{gauge boson} = \gamma^* \qquad \vec{q} = \vec{P}_1 - \vec{P}_2 = (\nu, \bar{q})$$

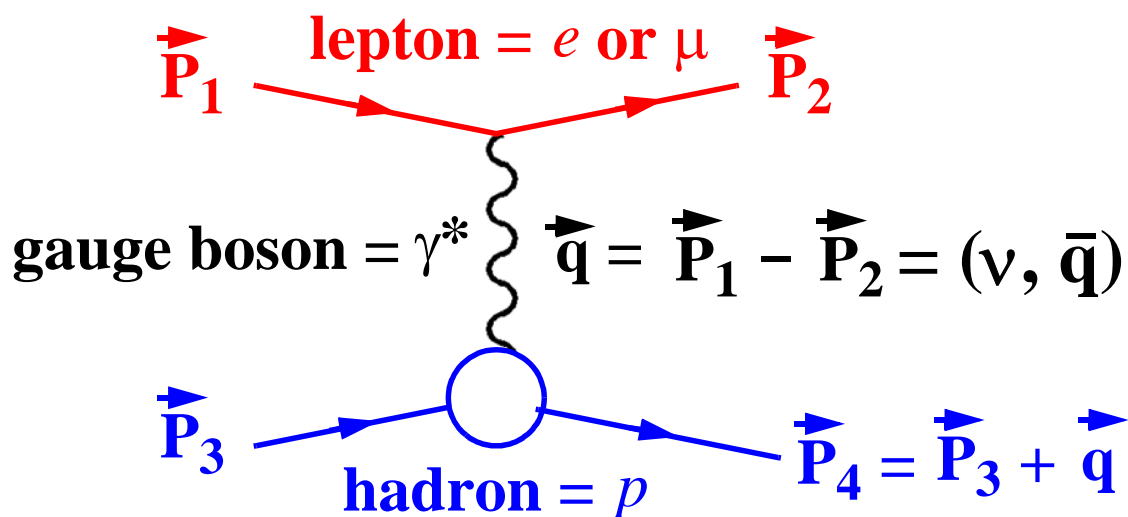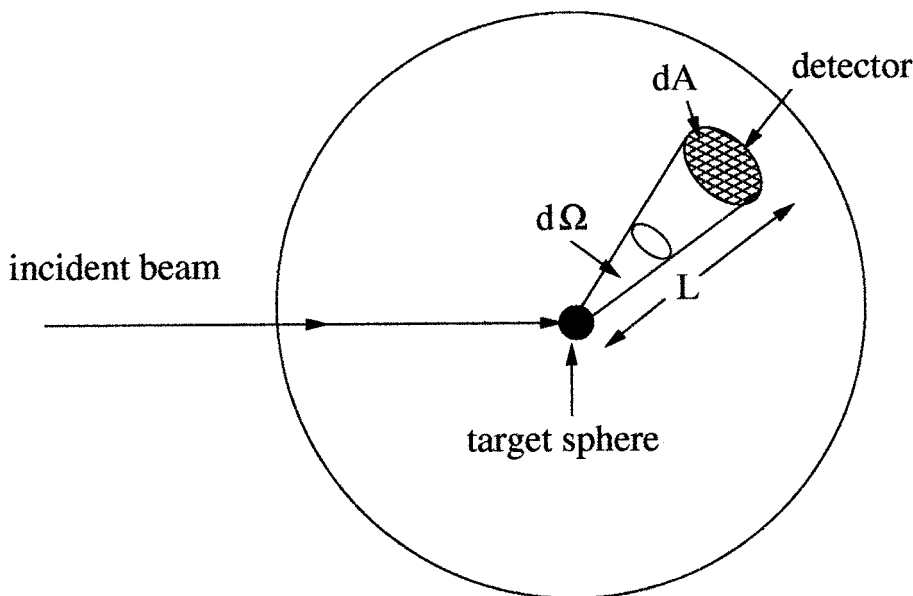$$\vec{P}_3 \qquad \textbf{hadron} = p \qquad \vec{P}_4 = \vec{P}_3 + \vec{q}$$

Figure 68:   The dominant one-photon exchange mechanism in elastic lepton-proton scattering.

❖   The angular distribution of the particles emerging from a scattering reaction is given by the differential cross-section

$$\frac{d\sigma(\theta, \varphi)}{d\Omega} \quad \text{where} \quad d\Omega \ = \ sin\,\theta\,d\theta\,d\varphi$$

$$d\Omega \ = \ \frac{dA}{L^2}$$

Figure 69: The definition of the solid angle $d\Omega$ in scattering experiments.

➔   The total cross section of the reaction is obtained by integrating the differential cross section:

$$\sigma = \int \frac{d\sigma(\theta, \varphi)}{d\Omega}\,d\Omega = \int_0^\pi \int_0^{2\pi} \frac{d\sigma(\theta, \varphi)}{d\Omega}\,sin\,\theta\,d\theta\,d\varphi$$
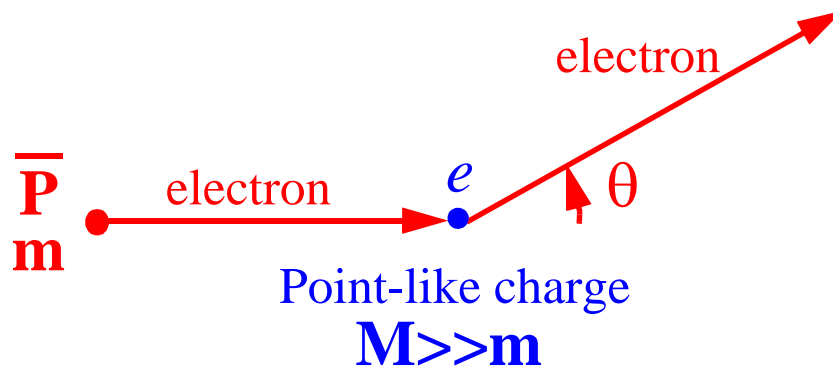
Figure 70: The scattering of an electron on a static point-like electrical charge.

➔   The angular distribution of a relativistic electron of momentum p which is scattered by a point-like static electric charge e is described by the Mott scattering formula:

$$\left(\frac{d\sigma}{d\Omega}\right)_M = \frac{\alpha^2}{4p^4 sin^4(\frac{\theta}{2})}\left(m^2 + p^2 cos^2\frac{\theta}{2}\right)$$

In the low energy limit $p<<m$, the Mott scattering formula is reduced to the non-relativistic Rutherford scattering formula:

$$\left(\frac{d\sigma}{d\Omega}\right)_R = \frac{m^2\alpha^2}{4p^4 sin^4(\frac{\theta}{2})} \qquad \text{where} \quad \alpha = \frac{e^2}{4\pi}$$

Static spherical
charge distribution

$e\rho(\bar{r})$

$\bar{r}$

$\overline{P}_1$ electron

electron $\overline{P}_2$

θ

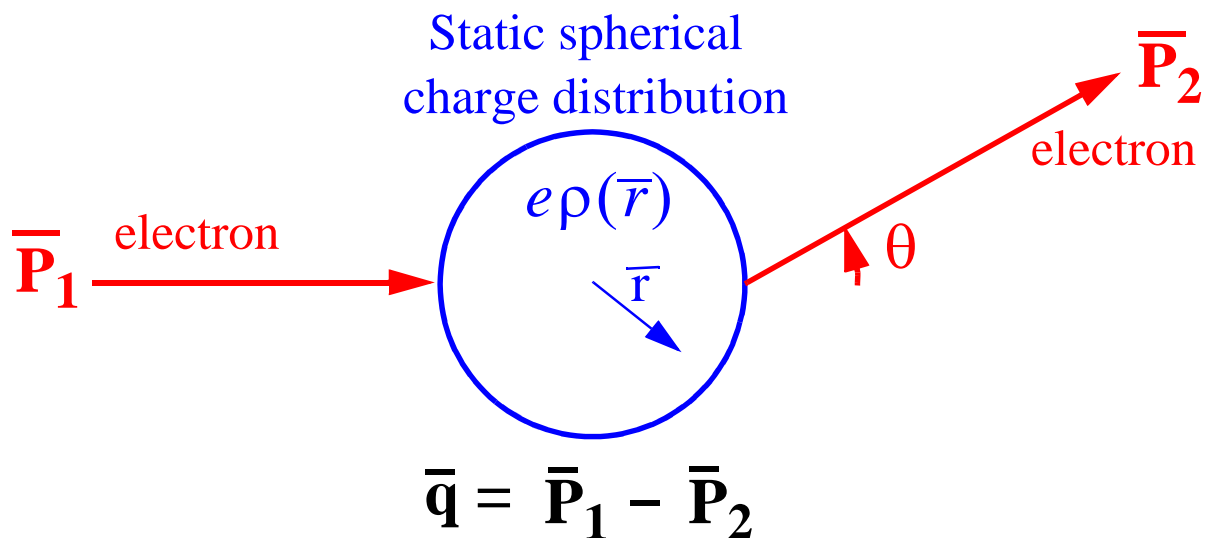$$\bar{q} = \overline{P}_1 - \overline{P}_2$$

Figure 71: The scattering of an electron on a static spherical charge distribution.

If the electric charge is not point-like, but it is spread out with a spherically symmetric density distribution, i.e., $e \rightarrow e\rho(r)$, where $\rho(r)$ is normalized:

$$\int \rho(r) d^3\bar{x} = 1$$

then the Rutherford scattering formula has to be modified by an electric form factor $G^2_E(q^2)$:

$$\frac{d\sigma}{d\Omega} = \left(\frac{d\sigma}{d\Omega}\right)_R G^2_E(q^2) \tag{89}$$

➔   The electric form factor is the Fourier transform of the charge distribution with respect to the momentum transfer $\bar{q}$:

$$G_E(q^2) = \int \rho(r)e^{i\bar{q} \cdot \bar{x}}d^3\bar{x} \qquad (90)$$

– For $q = 0$, $G_E(0) = 1$ (low momentum transfer)

– For $q^2 \to \infty$, $G_E(q^2) \to 0$ (large momentum transfer)

➔   Measurements of the cross-section can be used to determine the form-factor and hence the charge distribution.

The mean quadratic charge radius is for example given by

$$r_E^2 = \int r^2\rho(r)d^3\bar{x} = -6\frac{dG_E(q^2)}{dq^2}\bigg|_{q^2 = 0} \qquad (91)$$
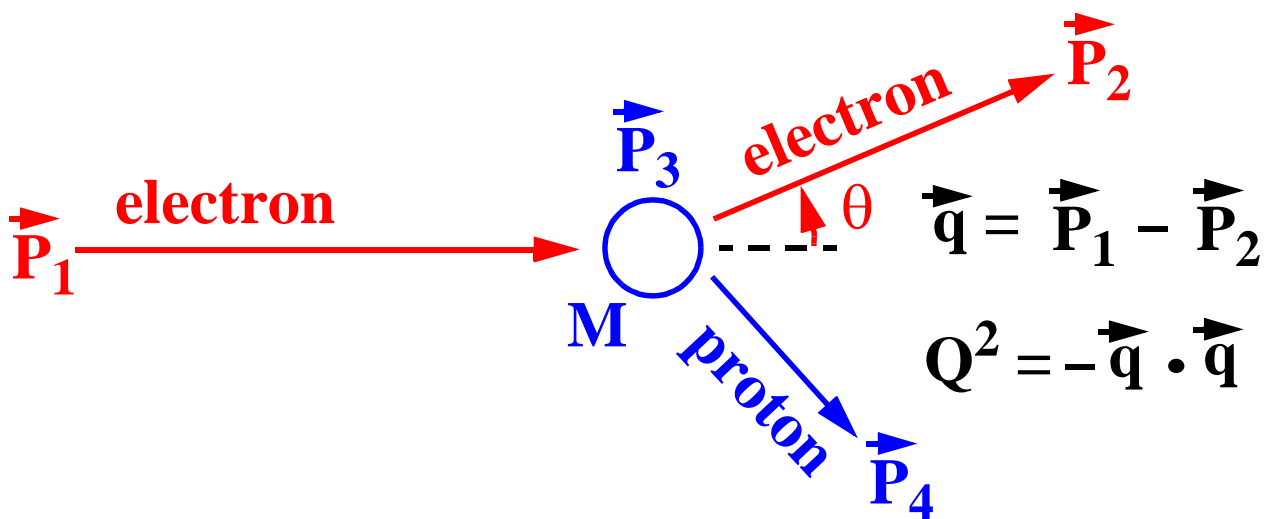
Figure 72: Elastic electron-proton scattering when the recoil energy of the proton is taken into account.

→ Scattering of electrons on protons depend not only on the electric form factor G_E but also on a magnetic form factor G_M which is associated with the magnetic moment distribution.

$$\frac{d\sigma}{d\Omega} = \left(\frac{d\sigma}{d\Omega}\right)_{\mathbf{M}} \times \left(G_1(Q^2)\cos^2\frac{\theta}{2} + \frac{Q^2}{2M^2}G_2(Q^2)\sin^2\frac{\theta}{2}\right)$$

$$G_1(Q^2) = \frac{G_E^2 + \frac{Q^2}{4M^2}G_M^2}{1 + \frac{Q^2}{4M^2}} \qquad G_2(Q^2) = G_M^2$$

➡️ Measurement of the form factors are conveniently divided into three Q^2 regions:

1) low $Q^2 \Rightarrow Q \ll M \Rightarrow G_E$ dominates the cross-section and r_E can be precisely measured:

$$r_E = 0,85 \pm 0,02 \ fm \tag{92}$$

2) An intermediate range: $0.02 \le Q^2 \le 3 \ \text{GeV}^2 \Rightarrow$ both G_E and G_M give sizeable contribution $\Rightarrow$ the result can be given by the parameterization:

$$G_E(Q^2) \approx \frac{G_M(Q^2)}{\mu_p} \approx \left(\frac{\beta^2}{\beta^2 + Q^2} \right)^2 \tag{93}$$

with β^2=0.84 GeV

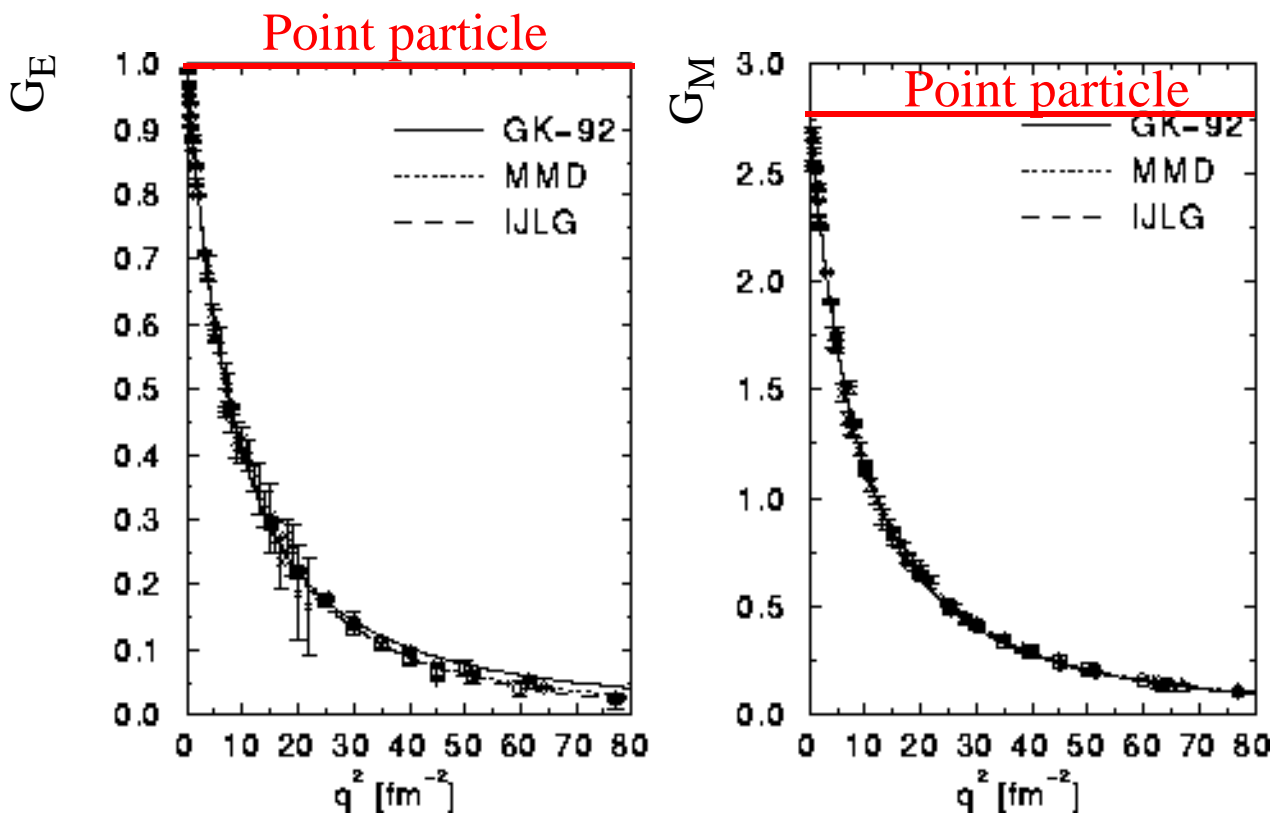3) high $Q^2 > 3 \ \text{GeV}^2 \Rightarrow G_M$ dominates the cross section:

Figure 73:   Electric and magnetic proton form-factors, compared with different parameterizations.

The form factors are normalized so that

$$G_E(0) = \text{total charge} \qquad = 1 \ (p)$$
$$= 0 \ (n)$$

$$G_M(0) = \text{magnetic moment} = \mu_p = +2.79 \ (p)$$
$$= \mu_n = -1.91 \ (n)$$

➔   If the proton is a point particle then

$$\mathbf{G_E(Q^2) = 1} \ \text{and} \ \mathbf{G_M(Q^2) = 2{,}79}$$

Inelastic lepton-proton scattering

❖   Inelastic electron-proton scattering can be used to probe the proton structure and gave the first evidence for the existence of quarks.

$$\vec{P}_1 \quad \xrightarrow{\text{electron}} \quad \vec{P}_2$$

$$\gamma^* \quad \vec{q} = \vec{P}_1 - \vec{P}_2 = (\nu, \bar{q})$$

$$M \qquad \vec{P}_4 = \vec{P}_3 + \vec{q}$$

$$\vec{P}_3$$

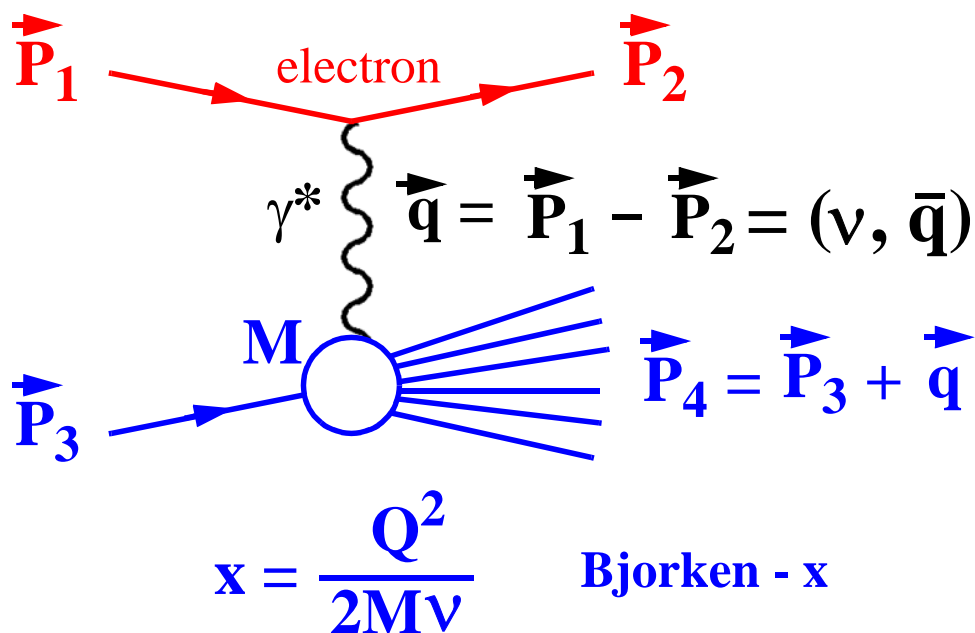$$x = \frac{Q^2}{2M\nu} \qquad \text{Bjorken - x}$$

Figure 74:   One-photon exchange in inelastic lepton-proton scattering.

➔   In inelastic lepton-proton scattering a new dimensionless variable called the Bjorken scaling variable x is introduced where $0<x<1$.

➔   The differential cross section for inelastic electron-proton scattering can be written as:

$$\frac{d\sigma}{dE_2 d\Omega} = \frac{\alpha^2}{4E_1^2 \sin^4\left(\frac{\theta}{2}\right)} \cdot \frac{1}{\nu} \cdot$$

$$\cdot \left[F_2(x, Q^2)\cos^2\left(\frac{\theta}{2}\right) + \frac{Q^2}{xM^2} F_1(x, Q^2)\sin^2\left(\frac{\theta}{2}\right) \right]$$

➔   The two dimensionless structure functions $F_1(x,Q^2)$ and $F_2(x,Q^2)$ parameterize the photon-proton interaction in the same way as $G_1(Q^2)$ and $G_2(Q^2)$ in elastic scattering.

➔   Bjorken scaling or scale invariance:

$$F_{1,2}(x, Q^2) \approx F_{1,2}(x)$$

i.e. for $Q \gg M$, structure functions are almost independent of Q^2. If all particle masses, energies and momenta are multiplied by a scale factor, structure functions at any given x remain unchanged.
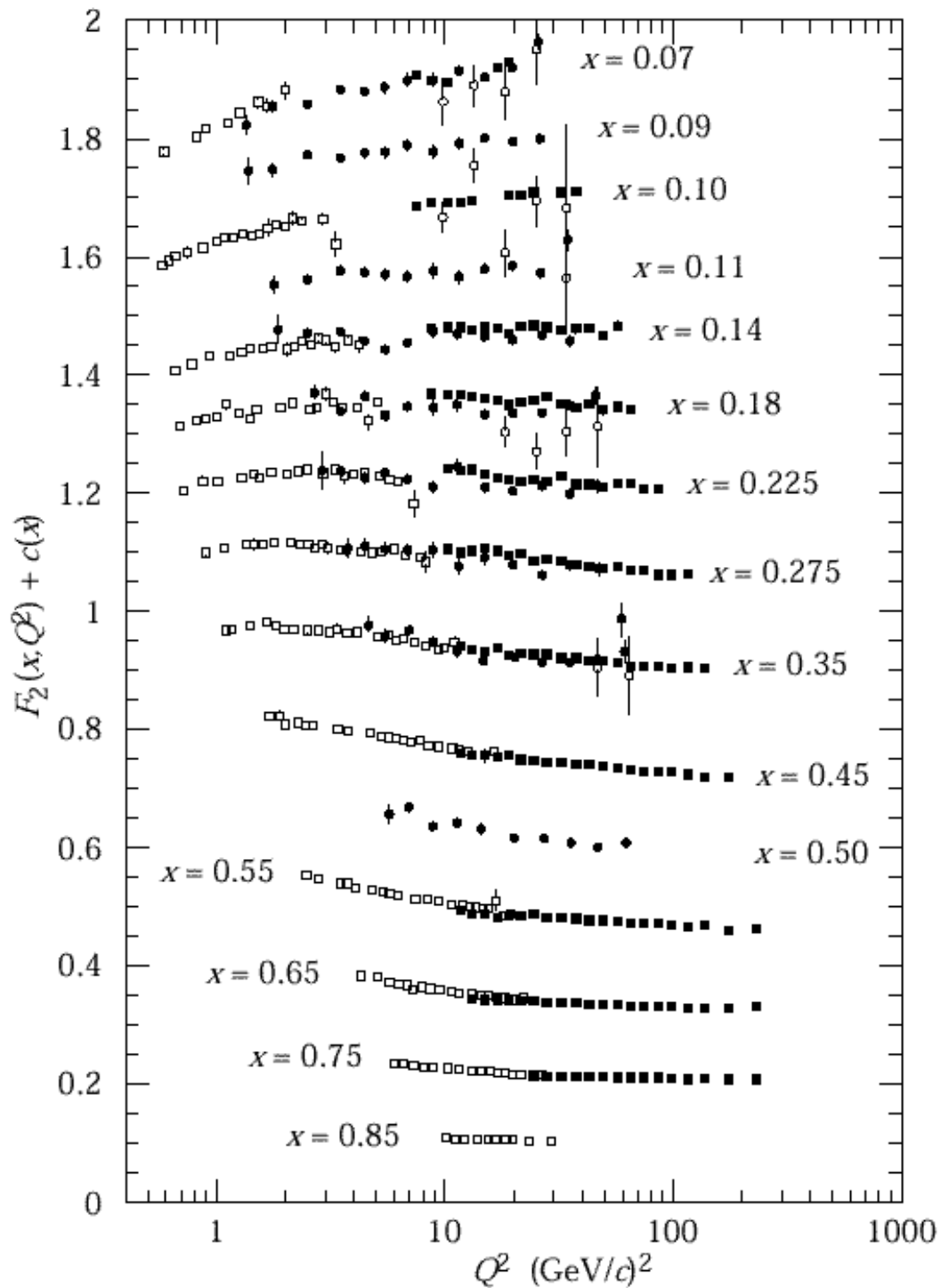
Figure 75: The measured structure function F_2 (compilation of data from different experiments).
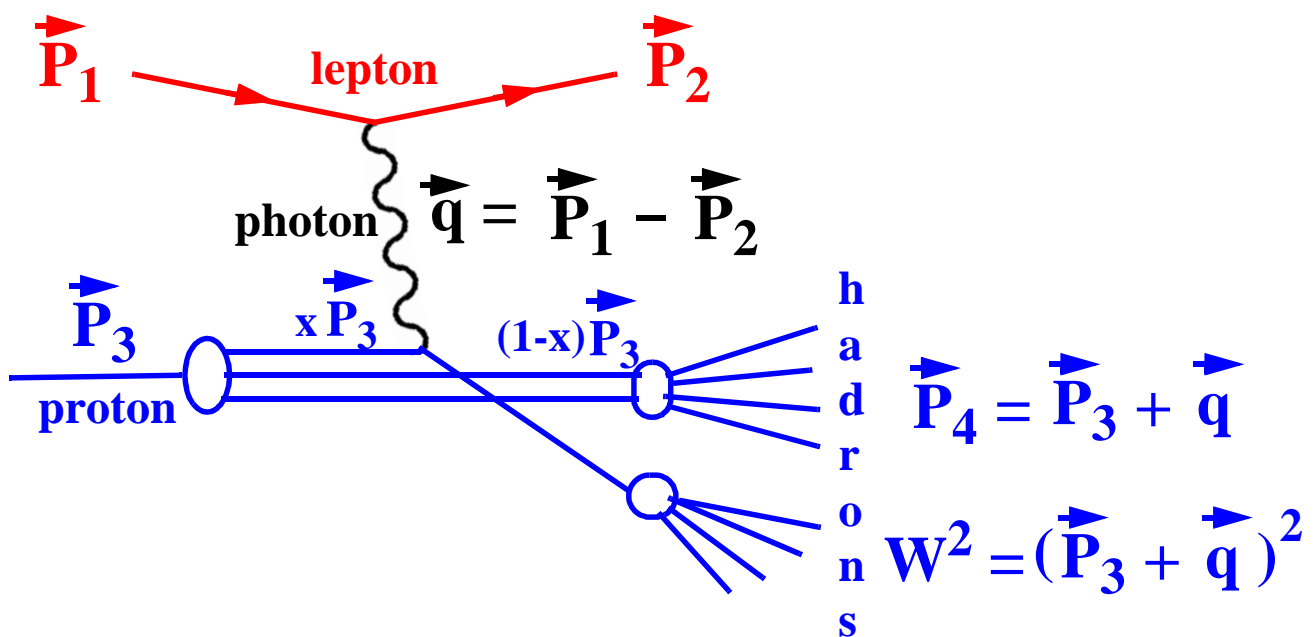
➔ The first observation of scale invariance in inelastic scattering was observed at SLAC in 1969 and was later interpreted as the first evidence for quarks.

Figure 76:   Two spectrometers in SLAC´s End Station A that were used to discover quarks in the late 1960s.

Deep inelastic electron-proton scattering.

❖   In the parton model the scale invariance is explained by scattering on point-like constituents (partons) in the proton.

$$\vec{P}_1 \quad \text{lepton} \quad \vec{P}_2$$

photon $\quad \vec{q} = \vec{P}_1 - \vec{P}_2$

$$\vec{P}_3 \quad x\vec{P}_3 \quad (1\text{-}x)\vec{P}_3 \quad \text{hadrons}$$

proton

$$\vec{P}_4 = \vec{P}_3 + \vec{q}$$

$$W^2 = (\vec{P}_3 + \vec{q})^2$$

➔   We now know that the partons in the parton model are identical to the quarks in the quark model.

➔   The parton model is valid if the target proton has a sufficiently large momentum, so that the fraction of the proton momentum carried by the struck quark is given by Bjorken x.
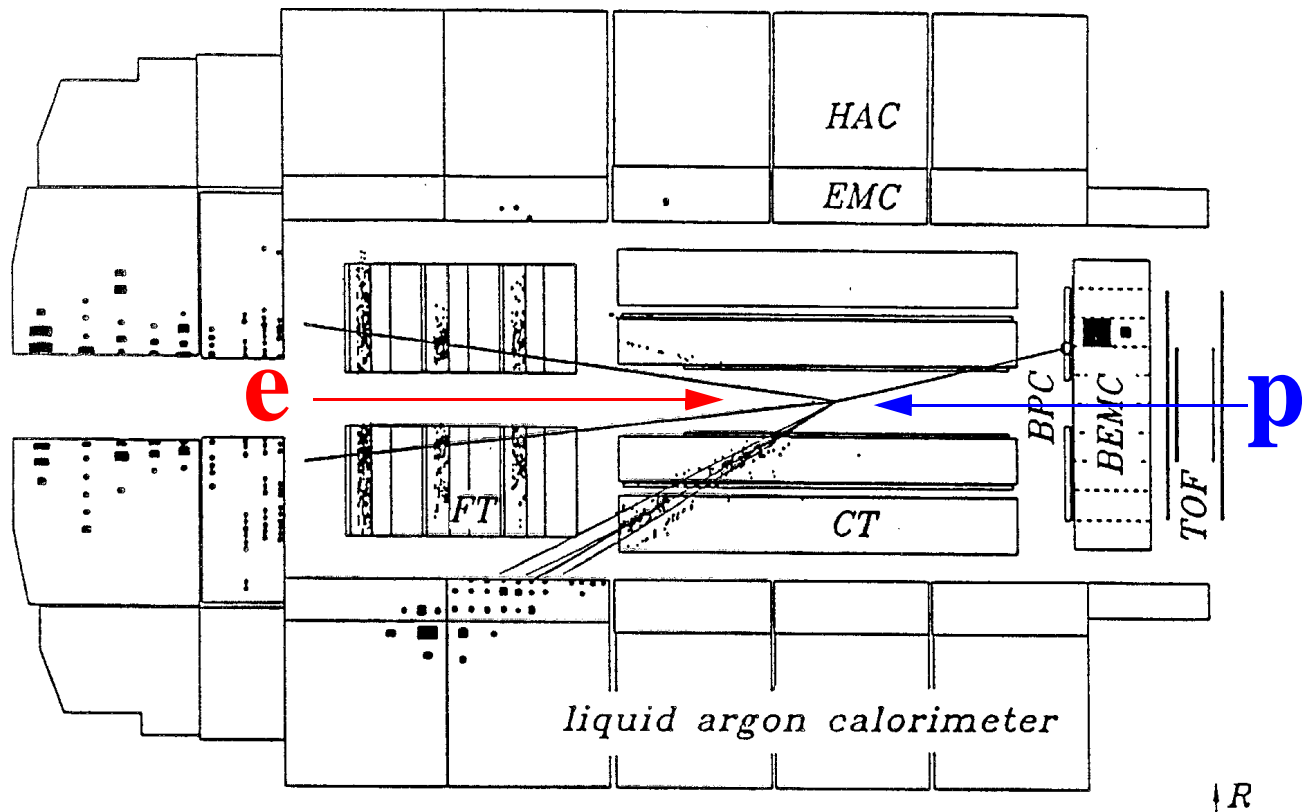
Figure 77:   A computer reconstruction of a deep inelastic electron-proton scattering event recorded by the H1 experiment at DESY.
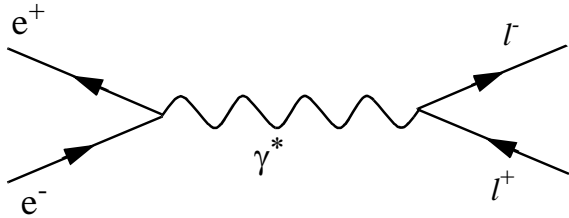
➔   In the parton model, the structure function F$_1$ depends on the spin of the partons:

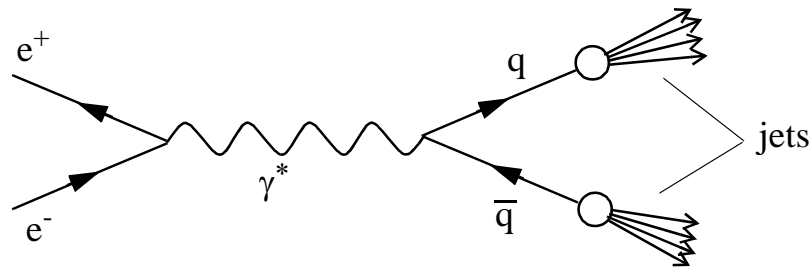$$F_1(x, Q^2) = 0 \qquad\qquad (spin\text{-}0)$$

$$2xF_1(x, Q^2) = F_2(x, Q^2) \qquad (spin\text{-}1/2)$$

The data favours the second relation (called the Callan-Gross relation) i.e. quarks have spin 1/2.
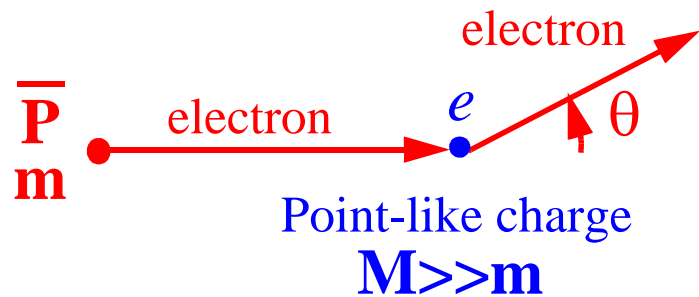
ELECTRON-POSITRON INTERACTIONS

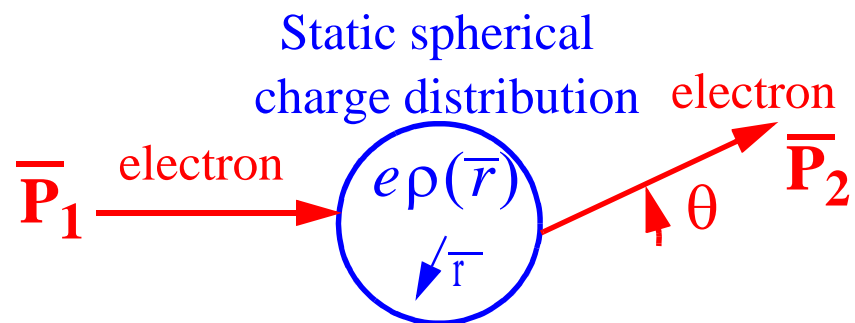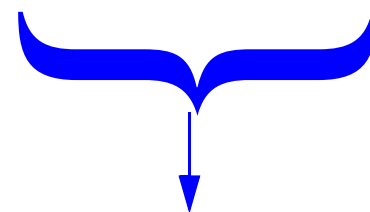$$\frac{d\sigma}{d\cos\theta}(e^+e^- \to l^+l^-) = \frac{\pi\alpha^2}{2Q^2}(1+\cos^2\theta)$$

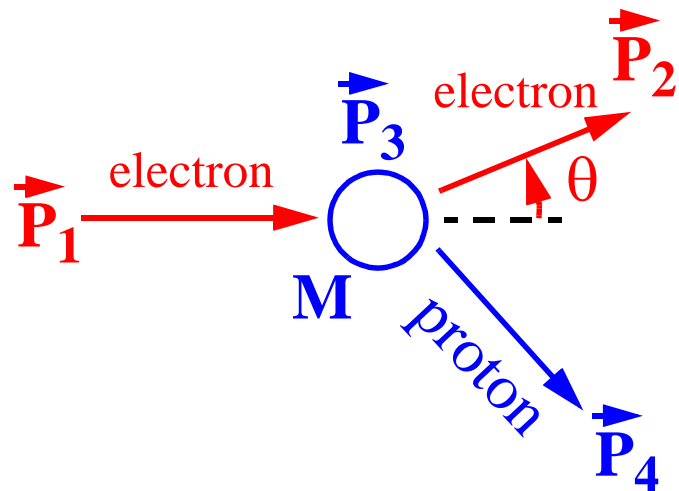$$\frac{d\sigma}{d\cos\theta}(e^+e^- \to q\bar{q}) = N_c e_q^2 \frac{\pi\alpha^2}{2Q^2}(1+\cos^2\theta)$$

ELASTIC ELECTRON-PROTON SCATTERING

electron

$\overline{P}$
m
electron
e
θ
electron

Point-like charge
M>>m

$$\left(\frac{d\sigma}{d\Omega}\right)_M = \frac{\alpha^2}{4p^4 \sin^4\left(\frac{\theta}{2}\right)}\left(m^2 + p^2\cos^2\frac{\theta}{2}\right)$$
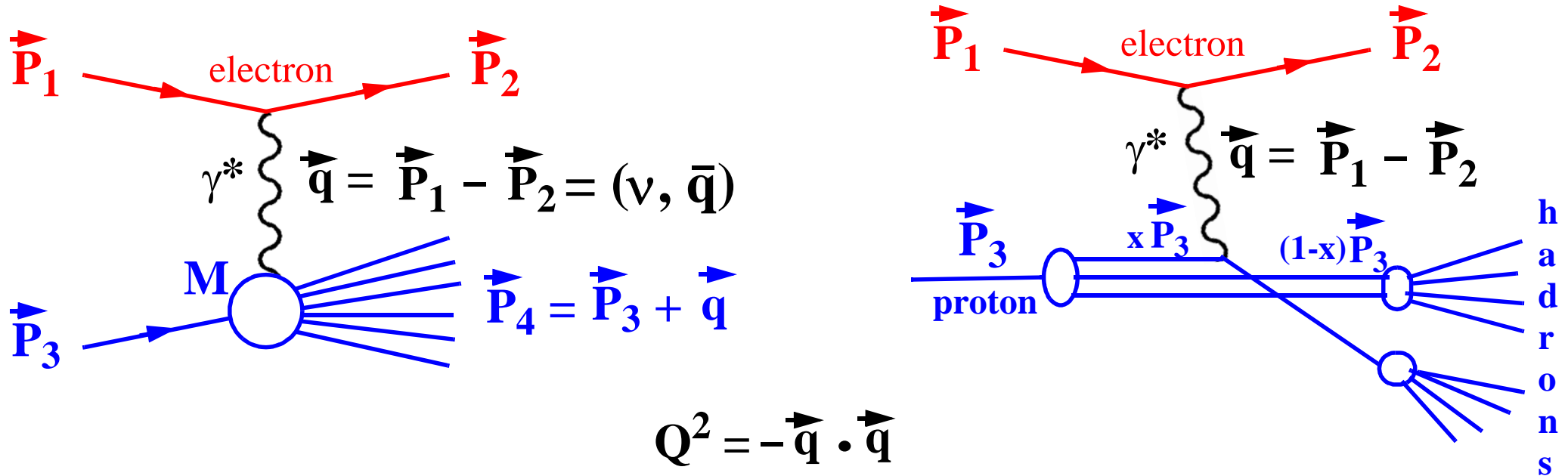
Static spherical
charge distribution

$\overline{P}_1$
electron
$e\rho(\overline{r})$
$\overline{r}$
electron
θ
$\overline{P}_2$

$$\frac{d\sigma}{d\Omega} = \left(\frac{d\sigma}{d\Omega}\right)_R G_E^2(q^2)$$

$\overrightarrow{P}_3$
$\overrightarrow{P}_2$
electron
$\overrightarrow{P}_1$
electron
θ
M
proton
$\overrightarrow{P}_4$

$$\frac{d\sigma}{d\Omega} = \left(\frac{d\sigma}{d\Omega}\right)_M \times \left(G_1(Q^2)\cos^2\frac{\theta}{2} + \frac{Q^2}{2M^2}G_2(Q^2)\sin^2\frac{\theta}{2}\right)$$

$$G_1(Q^2) = \frac{G_E^2 + \frac{Q^2}{4M^2}G_M^2}{1 + \frac{Q^2}{4M^2}} \qquad G_2(Q^2) = G_M^2$$

INELASTIC ELECTRON-PROTON SCATTERING

$$\vec{q} = \vec{P}_1 - \vec{P}_2 = (\nu, \vec{q})$$

$$\vec{P}_4 = \vec{P}_3 + \vec{q}$$

$$Q^2 = -\vec{q} \cdot \vec{q}$$

$$x = \frac{Q^2}{2M\nu} \quad \text{Bjorken - x}$$

$$\frac{d\sigma}{dE_2 d\Omega} = \frac{\alpha^2}{4E_1^2 \sin^4\left(\frac{\theta}{2}\right)} \bullet \frac{1}{\nu} \bullet \left[F_2(x, Q^2)\cos^2\left(\frac{\theta}{2}\right) + \frac{Q^2}{xM^2} F_1(x, Q^2)\sin^2\left(\frac{\theta}{2}\right) \right]$$

Summary

- ## Quantum Chromodynamics

  a) The gauge bosons in QCD are called gluons and are spin 1 particles.

  b) The charge in QCD is called colour and gluons carry colour charge but not electric charge.

  c) The strong interaction is flavour independent.

  d) Colour confinement means that a particle with a colour charge (such as a gluon or a quark) cannot exist as a free particle.

- ## The strong coupling constant.

  e) The strong coupling constant α_s gives the strength of the strong interaction.

  f) α_s is not a true constant since it depends on Q^2.

• **Electron-positron interactions.**

g) Quarks are seen as jets of hadrons in electron-positron interactions.

h) The measured cross section ratio R can only be explained if there are 3 colours.

i) A measurement of the angular distribution of jets in two-jet events show that the quark is a spin 1/2 particle.

j) Three-jet events can be used to measure α_s and to show that the gluon is a spin 1 particle.

• **Elastic electron-proton scattering.**

k) Elastic electron-proton scattering can be used to measure the size of the proton.

l) Scattering of electrons on protons depends on an electric and a magnetic form factor.

m) The measurement of these form factors show that the proton is not a point particle.

• Inelastic lepton-proton scattering.

n) Inelastic scattering of electrons on protons depends on two structure functions F_1 and F_2.

o) Scale invariance means that these structure functions are almost independent on Q^2. The scale invariance of F_2 is evidence for the existence of quarks in the proton.

• Deep inelastic electron-proton scattering.

p) The measurement of F_1 show that the quarks have to be spin 1/2 particles.